LABORATORY (AND ON-ORBIT) MAGNETOMETER CALIBRATION WITHOUT COIL FACILITIES OR ORIENTATION INFORMATION

Paul Graven
Ph.D. Candidate in Aeronautics and Astronautics
Stanford University
Stanford, CA

Thomas Kenny
Assistant Professor of Mechanical Engineering
Stanford University
Stanford, CA

Abstract

Magnetometer calibration is normally performed using shielded (or otherwise magnetically benign) coil facilities to provide a known uniform field. And measurements are taken with precise knowledge of sensor orientation. These facilities are expensive and can be tedious to use. A method for calibration based on field magnitude only has been developed. Accurate determination of relative orientations and relative scale factors between sensor axes requires only that the field magnitude be approximately constant. No coils or precision fixtures are needed. The method is extended to handle redundant sensitive axes, and fields of variable magnitude. The latter is of considerable interest, since it could be used to estimate drifts of scale factors or biases for instruments on-orbit.

1.0 Introduction

This paper presents a calibration method for vector magnetometers which yields relative orientations and relative scale factors between sensor axes without the need for magnetic field or sensor package orientation information. This allows calibration to be carried out in the laboratory without precision fixturing or costly magnetic environment facilities, provided that the noise environment is benign and field gradients are small. If the field magnitude is known, absolute scale factors can be found with a single additional element. In addition, if the direction and magnitude of the local magnetic field are known in the laboratory frame, absolute calibration can be obtained with two additional measurements. This methodology can be extended to sensors with redundant sensitive axes, and to on-orbit calibration of spacecraft magnetometers.

1.1 Current Practice

First the bias is determined by taking a measurement inside of a magnetically shielded region. Then a few measurements are taken with a known field strength and known orientations relative to the sensor package.* Three measurements, each with the field aligned along a different sensor axis will provide the necessary data for determining scale factors and relative alignment. The scale factor for a particular axis is given by

$$sf_i = \frac{m_i - b_i}{|B|}. \qquad (1)$$

Where m_i is the sensed output for the i^{th} axis, b_i is the bias for that axis and $|B|$ is the known field magnitude.

The relative orientations are determined from the outputs from the non-field-aligned axes for each measurement.

$$\cos(\alpha_{ij}) = \frac{m_j - b_j}{sf_j|B|}. \qquad (2)$$

Where α_{ij} is the angle between the i^{th} and j^{th} axis, and the i axis is the field aligned axis. This method assumes prior knowledge of the orientation of the sensor axes to within a degree or so. A better approach based on the same computational framework uses fine adjustments of the sensor package orientation to maximize the sensed output for the field aligned axis for each measurement.

Another potentially more accurate method uses least-squares to estimate the calibration parameters based on the measurement model

$$M_i = PB_i + b_M. \qquad (3)$$

Where M_i is the i^{th} measurement vector, P is the 3X3 matrix of calibration parameters, B_i is the magnetic field vector for the i^{th} measurement, and b_M is the vector of sensor biases.[1] Assuming the bias has been determined as above, the cost function to

*Based on observations of magnetometer calibration procedures at Applied Physics Systems in Mountain View, CA.

be minimized over the elements of P is given by

$$C=\sum_{i=1}^{n}\left(\hat{P}B_i-(M_i-b_M)\right)^2 . \qquad (4)$$

Where n is the number of measurements, and $\hat{P}$ is the estimated matrix of calibration parameters. The Scale factor estimates are the magnitudes of the vectors constituting the rows of $\hat{P}$, and the orientations are given by the directions of those vectors.

The main problems with these methods are cost and availability of facilities. A magnetically shielded workspace is needed for bias determination. A set of Helmholtz coils (preferably shielded) is needed for generation of precise, steady, and uniform fields for testing. And precision fixtures are needed for mounting and orienting the instruments to be calibrated.

1.2 Coordinate Measuring Machine Calibration

The method described is based on a procedure developed for calibration of coordinate measuring machines by Juoy and Clement.[2] A series of measurements are taken of a bar, with each measurement carried out with the bar in a different orientation. Calibration is accomplished by exploiting the orientation independence of the length of the bar. Each measurement produces a measurement vector

$$X=[x_1 \quad x_2 \quad x_3]^T \qquad (5)$$

whose length D is given by

$$D^2=X^T[g_i]X \qquad (6)$$

where $[g_i]$ is the 3x3 metric tensor. Since $[g_i]$ is symmetric there are six parameters to be identified. These parameters can be found by minimizing the objective function

$$C=\sum_{i=1}^{N}(X_i^T[g_{ij}]X_i-D^2)^2 \qquad (7)$$

where N is the number of measurements taken. For this formulation the relative scale factors are given by

$$Sf_i=\sqrt{\frac{g_i}{g_j}}, \qquad (8)$$

and the relative orientation angles are given by

$$\cos(\alpha_{ij})=\frac{g_{ij}}{\sqrt{g_{ii}\bullet g_{jj}}}. \qquad (9)$$

If D is known, the absolute scale factors are given by

$$Sf_i=\sqrt{g_{ii}}. \qquad (10)$$

A similar approach can be used to identify magnetometer scale factors and orientations, but as we shall see it is somewhat more complicated.

2. Theory

This section describes the approach developed for magnetometer calibration. For a magnetometer the output is proportional to the dot product of the field and the unit vector along the sensor axis. In contrast, for the coordinate measuring machine the output is the coordinates of the bar in the frame defined by the measurement axes. This distinction is illustrated in Figure 1*, where the ei are unit vectors, and $\mathbf{B}$ represents the bar for the coordinate measuring machine case, and the magnetic field vector for the magnetometer case.

First we formulate the optimization for the non-redundant case: 3-D with three sensors axes. For a particular measurement a simple model for magnetometer output is

$$M_i=\begin{bmatrix} m_{1i} \\ m_{2i} \\ m_{3i} \end{bmatrix}=P_0T_iB+v_i, \qquad (11)$$

where B is the true constant magnetic field vector, T_i is the 3x3 orthonormal rotation matrix representing the orientation of the sensor package for the i^{th} measurement, v_i is a measurement noise vector, and

$$P_0=\begin{bmatrix} S_1 \\ S_2 \\ S_3 \end{bmatrix} \qquad (12)$$

is the 3X3 matrix consisting of row vectors S_j which transform B into sensor outputs. The magnitude of S_j can be interpreted as the scale factor for the j^{th} sensor, and the direction of S_j can be interpreted as the orientation of the j^{th} sensor in the sensor package frame. It is these S_j we wish to identify for calibration.

To estimate P_0, as in the coordinate measuring machine case, we exploit the fact that the magnitude of B is constant. An estimate of B is given by

$$\hat{B}=T_i^{-1}\hat{P}^{-1}M_i \qquad (13)$$

* Adapted from Reference 1, p. 27.

Comparison of Sensor Outputs

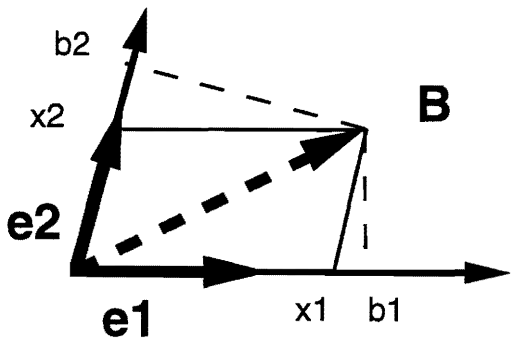

For the magnetometer the output is proportional to [b1 b2].

For the coordinate measuring machine the output is proportional to [x1 x2].

Figure 1

where $\hat{P}$ is the estimated P_0. The magnitude squared of $\hat{B}$ then is given by

$$\hat{B}^2 = M_i^T \hat{P}^{-T} T_i^{-T} T_i^{-1} \hat{P}^{-1} M_i = M_i^T \hat{P}^{-T} \hat{P}^{-1} M_i. \quad (14)$$

As expected, the magnitude of $\hat{B}$ is independent of orthonormal transformations $(T_i^{-T} T_i^{-1} = I)$. Interestingly, this also illustrates the fact that any orthonormal transformation (rotation) of $\hat{P}$ will also be a solution since orthonormal transformations drop out of the equation for $\hat{B}^2$. This fact will be exploited later to simplify the parameter estimation problem.

From (14) this least-squares cost function can be generated for estimation of the elements of P:

$$C = \sum_{i=1}^{n} \left(M_i^T \hat{P}^{-T} \hat{P}^{-1} M_i - B\right)^2. \quad (15)$$

We now move from theory to practice.

3.0 Verification

In this section the methodology and results of the computer based* and experimental verification will be presented. Section 3.1 discusses the practical details of the estimation methods. Section 3.2 discusses data generation and estimation results using simulated data. Section 3.3 discusses data generation and estimation results using experimental data.

3.1 Identification Methodology

This section details the methods used to identify the elements of P_0. Two 3-D sensor configurations are developed. The first is based on a standard 3-axis magnetometer (three nominally orthogonal measurement axes) and P_0 is 3x3, The second is based on two two-axis ring core fluxgate sensors (two sets of two nominally orthogonal sensor axes) and P_0 is 4x3. The second configuration is singly redundant.**

The basic development is the same for both configurations, however, the redundant case presents some practical difficulties which will be discussed in Section 4.1.

We begin with a more realistic version of measurement equation (11):

$$M_i = P_0 T_i (B_0 + v_{Bi}) + v_{Mi} + b_M \quad (16)$$

where P_0 is the matrix of sensor axis calibration vectors in the sensor package frame, T_i is the rotation matrix for transformations from the laboratory frame to the sensor package frame, B_0 is the nominal magnetic field vector in the laboratory frame, v_{Bi} is the magnetic field noise, v_{Mi} is the measurement noise, and b_M is the magnetometer bias. The noise vectors are assumed to have zero mean gaussian components.

Equation (16) can be solved for B_0, yielding

$$B_0 = T_i^{-1} P_0^{-1} \left(M_i - b_M - v_{Mi}\right) - v_{Bi}. \quad (17)$$

---

* All analyses were performed using Matlab™3 on a Sun Microsystems Sparc2 or an Apple Macintosh Centris 610 with a 40 MHz 68040 processor.

** It has one more sensitive axis than is required to span the space (four sensor axes in three dimensions).

If we then take the inner product of (17) with itself (square it), we obtain

$$
\begin{aligned}
B_0^2 &= M_i^T P_0^{-T} T_i^{-T} T_i^{-1} P_0^{-1} M_i + b_M^T P_0^{-T} T_i^{-T} T_i^{-1} P_0^{-1} b_M \\
&\quad + v_{Mi}^T P_0^{-T} T_i^{-T} T_i^{-1} P_0^{-1} v_{Mi} + v_{Bi}^T v_{Bi} \\
&\quad - 2 M_i^T P_0^{-T} T_i^{-T} T_i^{-1} P_0^{-1} b_M - 2 M_i^T P_0^{-T} T_i^{-T} T_i^{-1} P_0^{-1} v_{Mi} \\
&\quad + 2 b_M^T P_0^{-T} T_i^{-T} T_i^{-1} P_0^{-1} v_{Mi} - 2 v_{Bi}^T T_i^{-1} P_0 \left(M_i - b_M - v_{Mi}\right)
\end{aligned}
\tag{18}
$$

Noting that $T_i^{-T} T_i^{-1} = I$ and taking the expected value we obtain

$$
\begin{aligned}
E\left(B_0^2\right) &= E\left(M_i^T P_0^{-T} P_0^{-1} M_i\right) + E\left(b_M^T P_0^{-T} P_0^{-1} b_M\right) \\
&\quad + E\left(v_{Mi}^T P_0^{-T} P_0^{-1} v_{Mi}\right) + E\left(v_{Bi}^T v_{Bi}\right) - 2E\left(M_i^T P_0^{-T} P_0^{-1} b_M\right),
\end{aligned}
$$

or

$$
= E\left(M_i^T P_0^{-T} P_0^{-1} M_i\right) - 2E\left(M_i^T P_0^{-T} P_0^{-1} b_M\right) + CONST \,. \tag{19}
$$

So, the expected value of B_0^2 based on the measurement model from (16) is biased due to the squared noise and measurement bias terms. This will introduce an upward bias in the absolute scale factor estimates because it appears in (19) as a constant magnitude error in the expected value of B_0^2. It will not, however, impact estimates of relative orientations, or relative scale factors

To estimate P_0 and b_M. we minimize the objective function

$$
C = \sum_{i=1}^{N} \left(\sqrt{M_i^T \hat{P}^{-T} \hat{P}^{-1} M_i - 2 M_i^T \hat{P}^{-T} \hat{P}^{-1} \hat{b}_M} - \sqrt{B_0^2} \right)^2 \tag{20}
$$

or

$$
C = \sum_{i=1}^{N} \left(\sqrt{M_i^T \hat{P}^{-T} \hat{P}^{-1} M_i - 2 M_i^T \hat{P}^{-T} \hat{P}^{-1} \hat{b}_M} - 1 \right)^2 \tag{21}
$$

over the elements of $\hat{P}$ and $\hat{b}_M$, the estimated calibration matrix and measurement bias vector. B_0^2 from (20) can be replaced by 1 in (21) without-loss-of-generality because as we have seen, the relative orientations and relative scale factors are magnitude independent. It is only the absolute scale factor which depends on knowledge of B_0^2.* For simplicity in the remainder of this paper we will work with the objective function from (21).

For the three axis magnetometer $\hat{P}$ is 3x3 and $\hat{b}_M$ is 3x1 so there are nominally 12 parameters to be identified. Recalling that the objective function (21) is independent of orthonormal transformations of $\hat{P}$, the problem can be simplified (without loss in generality) by constraining the solution to a particular orientation. This is accomplished by using a $\hat{P}$ of the form

$$
\hat{P} = \begin{bmatrix} P_{11} & 0 & 0 \\ P_{21} & P_{22} & 0 \\ P_{31} & P_{32} & P_{33} \end{bmatrix} \tag{22}
$$

rather than

$$
\hat{P} = \begin{bmatrix} P_{11} & P_{12} & P_{13} \\ P_{21} & P_{22} & P_{23} \\ P_{31} & P_{32} & P_{33} \end{bmatrix} \tag{23}
$$

This greatly simplifies the problem by eliminating redundant solutions, and reducing the number of parameters to identify from 12 to nine. They can be further reduced to six if it is assumed that the bias is determined independently as described in Section 1.1.

3.2 Results Using Simulated Data

This section presents the data generation methodology, and estimation results using simulated data.

3.2.1 Data Generation

All simulated magnetometer data were generated within the Matlab™3 environment. Magnetic field data were simulated by generating random vectors composed of zero mean gaussian components, and normalizing each vector to unit magnitude. To these randomly oriented unit vectors, zero mean gaussian noise vectors were added to simulate various levels of field and sensor noise. Then the simulated magnetic field data were transformed to simulated measurements through multiplication by P_0 and addition (if necessary) of the bias terms.

3.2.2 Estimation Results

The Matlab™ function leastsq** was used to determine the parameter set that minimized (21) using $\hat{P}$ from (22) and the simulated data. To begin the optimization, initial guesses of the elements of $\hat{P}$ are within 20% of the elements P_0. All but the noisiest of cases converged to near the true parameters independent of the quality of the initial guess. Convergence problems for 30 measurements begin to appear at noise levels around 10% of the mean field strength.

---

* The absolute scale factor is easily determined from a single measurement of a field with a precisely known magnitude once the relative calibration parameters are known.

** See the Matlab™3 Optimization Toolbox manual for a detailed description of the leastsq function.

Estimation Results with Simulated Data (three-axis magnetometer)

Number of Measurements	Measurement Noise (%)	Scale Factor Error (%)		Orientation Error (deg.)		Bias Error (%)	
		mean	std. dev.	mean	std. dev.	mean	std. dev.
30	1.2	0.0380	0.5300	0.0630	0.4850	NA	NA
120	1.2	0.0240	0.2800	-0.0180	0.2660	NA	NA
480	1.2	0.0260	0.1400	0.0005	0.1260	NA	NA
1000	1.2	0.0071	0.0900	0.0094	0.0870	NA	NA
480	3.0	0.1500	0.3200	0.0210	0.2970	NA	NA
480	0.3	-0.0026	0.0360	0.0028	0.0296	NA	NA
30	1.2	0.0504	0.5000	-0.0550	0.4700	0.0130	0.3600
120	1.2	0.0160	0.2700	0.0028	0.2570	0.0170	0.2100
480	1.2	0.0270	0.1400	0.0120	0.1200	-0.0058	0.1000
1000	1.2	0.0320	0.0980	-0.0002	0.0770	-0.0071	0.0680
480	3.0	0.1700	0.3600	0.0120	0.3000	-0.0210	0.2400
480	0.3	0.0025	0.0320	0.0019	0.0320	-0.0010	0.0250

Table 1

Some results are summarized in Table 1. Fifty independent runs were performed for each case to obtain the statistics. The scale factor error and bias error results are shown as percent of mean field magnitude.

As can be seen the method works, and is statistically well behaved. All of the estimation runs converged to the neighborhood of the desired solution (see the mean error columns). Standard deviations scale approximately inversely with the square root of the number of samples, and linearly with the noise standard deviation. There is little difference between the accuracy of the results for runs with bias estimation and those without.

These results will be used to support interpretation of the experimental results in the next section.

3.3 Experimental Results

This section details the data collection methods and estimation results for the experimental data.

3.3.1 Data Collection

Experimental data were collected using a laptop based data acquisition system. One set of data was taken in a relatively noisy, high field gradient laboratory environment, and the other was taken outdoors on a lawn at least 30 meters from buildings and lights to achieve lower noise and smaller field gradients. They will be referred to as the *lab* and the *outside* data sets respectively.

Each data set consists of 1000 samples from each axis taken at 10 Hz. To ensure that all of the sensor axes were sufficiently exercised, the sensor was rotated multiple times about numerous axes *by hand* within a region approximately one foot on a side. The computer and power supply were approximately two meters from the sensor during data gathering. (Remember, part of the goal of this research is to minimize the need for expensive fixtures, facilities and procedures.)

The sensor tested was an Applied Physics Systems APS533 miniature 3-axis fluxgate magnetometer. According to the product literature: it has a range of ±1 gauss at 4 volts/gauss; it's noise level is 10^{-6} gauss RMS./$\sqrt{Hz}$; the initial bias is less than 0.01 volts, and orthogonality between axes is ±2.0°.

The bias of the instrument was determined in a magnetically shielded chamber to be

$$b_{APS533} = \begin{bmatrix} 0.0069 \\ -0.0333 \\ 0.0118 \end{bmatrix} \qquad (24)$$

by averaging 1000 samples.

Estimation Results with Experimental Data (APS533 three-axis fluxgate magnetometer)

Data Set	Number of Measurements	Scale Factor Estimates x	Scale Factor Estimates y	Scale Factor Estimates z	Relative Alignment Estimates x-y	Relative Alignment Estimates y-z	Relative Alignment Estimates x-z	Bias Estimates x	Bias Estimates y	Bias Estimates z
lab	120	1.006	1.000	1.013	0.269	2.867	1.829	NA	NA	NA
lab	480	1.004	0.998	0.998	0.221	1.627	0.598	NA	NA	NA
outside	30	1.942	1.964	1.942	0.170	1.005	0.514	NA	NA	NA
outside	120	1.944	1.947	1.950	0.143	1.132	0.514	NA	NA	NA
outside	480	1.944	1.945	1.949	0.198	1.089	0.506	NA	NA	NA
outside	1000	1.944	1.945	1.947	0.240	1.121	0.493	NA	NA	NA
lab	120	1.013	1.001	1.002	0.247	3.082	0.549	0.0219	-0.035	0.031
lab	480	1.010	0.998	0.999	0.250	1.690	0.805	0.0153	-0.0342	0.0117
outside	30	1.942	1.968	1.935	0.197	1.075	0.407	0.0084	-0.03	0.0187
outside	120	1.945	1.946	1.948	0.139	1.108	0.507	0.0079	-0.0361	0.0102
outside	480	1.944	1.944	1.948	0.173	1.073	0.510	0.0074	-0.0355	0.0107
outside	1000	1.944	1.944	1.945	0.221	1.100	0.498	0.0069	-0.0351	0.0104

Table 2

3.3.2 Estimation Results

The experimental data were processed using the same methods that were used with the simulated data. For meaningful comparison with the simulation results a few statistics are needed regarding the magnitude of the experimental data sets:

Lab mean	0.998 V
Lab noise	3.0 %
Outside mean	1.947 V
Outside noise	1.2 %.

This indicates that the mean field strength for the lab data set was ~0.25 gauss compared with ~0.5 gauss for the outside data set.

Table 2 shows the estimation results. Scale factor estimates are in volts* , relative alignment estimates are in degrees from orthogonal, and bias estimates are in volts. The first six rows are results of the optimization with the measured bias subtracted from the data and no bias estimation. For the second six rows the raw data is used, and the bias is estimated.

The first thing to notice is that except for the biases the estimates are within the manufacturers specifications. The orthogonality comes in at better than 2 degrees, and scale factors are within 0.2% of each other for the best estimates (outside with 1000 measurements). The estimated biases are within 10% of the measured values.

We can now look to the simulated results (Table 1) to examine the accuracy of the results. For 1000 measurements and 1.2% noise we should expect scale factor estimates to have a standard deviation of ~0.1%, orientation angle estimates to have a standard deviation of ~0.08 degrees, and bias estimates to have standard deviations of ~0.07%. The implications of this for the results from the last row of Table 2 are: 95% confidence that the scale factor estimates are within ±0.0039 volts; 95% confidence that the orthogonality estimates are within ±0.16 degrees, and 95% confidence that the bias estimates are within ±0.0027 volts. For the biases the measured results are all within the 95% confidence interval for the estimates.

With more measurements and/or less noisy data, significantly greater accuracy could be achieved.

4.0 Continuing Work

This section discusses two areas where some preliminary results have been obtained, and further work needs to be done. In Section 4.1 the implications of adding a redundant sensor axis are examined, and in Section 4.2 applications to on-orbit calibration are explored.

4.1 Singly Redundant Sensors

Interest in the four axis case stems from use of ring core fluxgate sensors.[4] A single ring core fluxgate sensor has two nominally orthogonal sensitive axes. Since it takes two of them to get a

*To find the absolute scale factors (volts/gauss) each relative scale factor estimate is divided by the measured field magnitude.

three axis measurement, it appeared that it might be interesting to extend the methodology to produce consistent, unbiased parameter estimates for all four axes in the singly redundant case.

It is a more difficult problem than it first appears. In this case $\hat{P}$ is 4x3, and the $\hat{P}^{-1}$ required in (17)-(21) is no longer uniquely related to $\hat{P}$. So, the method from Section 3 cannot be applied directly.

Thus far, the only workable solution, inelegant and inefficient as it may be, is to sequentially solve each combination of three axes* using the techniques from Section 3, and average the results. As would be expected, the simulation results are similar to the results from Table 1. An experimental instrument is under construction.

More elegant methods of resolving this problem are being explored

4.2 On-Orbit Calibration.

There are three fundamental approaches which can be taken to explore the applicability of the method to on-orbit calibration. In the first, we assume knowledge of the field magnitude from magnetic field models. In this case the data can be normalized and the analysis can proceed as in Section 3. The main limitation is the accuracy of the models, and knowledge of spacecraft location. In LEO on magnetically quiet days typical RMS. magnitude errors due to field variability and model errors are ~0.5%[5]. This indicates that very accurate calibration could be accomplished if the noise and induced fields from the spacecraft are small at the sensor location. Simulations with historical spacecraft data need to be done.

The second approach applies the methods of Section 3 directly to the on-board measured data with out compensation for magnitude variation. It converges for random fields of variable magnitude, however, extremely large numbers of measurements are required. The scaling can be extrapolated from the results in Table 1. For 0.3% and 0.3 degrees RMS. accuracy with an RMS field strength variation of 30% approximately 50000 measurements are needed (it can be done). Work is in process to explore the limitations and applications of the method for on-orbit calibration. Preliminary work has shown that differences in the variability of the field among sensor axes (as a spacecraft might experience) tend to reduce the accuracy of the method.

Other potential approaches involve real-time or batch filtering of magnetometer and other sensor or dynamics information. Interesting related work has been performed by Psiaki[6] and by Lerner and Shuster.[7] Psiaki assumes he has a calibrated on-board magnetometer (and star sensor) and estimates orbit and field model parameters. Lerner and Shuster estimate magnetometer bias and spacecraft attitude based on magnetometer and other attitude data.

* If all combinations are not used the results will be biased because the data for each axis won't be used the same number of times, and consequentially data from some axes will effectively be weighted more heavily than that from others.

5. Conclusions

A method of magnetometer calibration has been developed which does not require knowledge of the magnitude or orientation of the magnetic field to determine relative scale factors, biases and alignments (orthogonality). The method is based on minimizing the error between a field of unit magnitude and an estimated field magnitude based on the measured data.

The estimation results using simulated data show that the method is statistically well behaved, and provide a basis for evaluating the experimental results.

Experiments with a high quality, commercially available magnetometer show that a calibration more accurate than the manufacturers published specifications could be performed in the field in a few minutes time with a laptop computer. For the experimental instrument 1000 samples gathered in 100 seconds with a magnitude noise standard deviation of ~1%, relative scale factors and biases were found to within 0.1% of the nominal field magnitude and orthogonality was determined to within 0.1 degrees.

This method seems to be a very good candidate for on-orbit calibration of spacecraft magnetometers. Further work needs to be done.

6. Acknowledgments

TRW, Inc. generously supported this research through a grant and fellowship from the Space and Electronics Group.

Gravity Probe B, and Stanford's OPAL project loaned the APS533 magnetometer for experiments.

Bill Goodman of Applied Physics Systems patiently fielded many questions, and demonstrated their calibration methods.

Many thanks to Professor Daniel DeBra from Stanford and his spacecraft research group for their input and early support in this effort.

7. References

[1] Vincent, S., *Design of a Feedback Controlled Magnetic Environment Chamber,* Unpublished Manuscript, Stanford University, Aug. 1992.

[2] Juoy, F., and Clement, A., *Theoretical Modelisation and Experimental Identification of the Geometrical Parameters of Coordinate-Machines by Measuring a Multi-Directed Bar,* Annals of the CIRP, Vol. 35/1/1986, pp. 393-396.

[3] The Math Works , Inc., *Matlab Reference Guide*, The Math Works, Inc., Natick, MA, 1995.
[4] Acuna, M. and Pellerin, C., *A Miniature Two-Axis Fluxgate Magnetometer*, IEEE Trans. Geosci. Electronics, V. GE-7, No. 4, pp. 252-260, 1969.
[5] Wertz,J.R. ed., *Spacecraft Attitude Determination and Control*, D. Reidel Pub. Co., Boston, 1978.
[6] Psiaki, M.L., *Autonomous Orbit and Magnetic Field Determination Using Magnetometer and Star Sensor Data*, AIAA Paper No. 93-3825, 1993.
[7] Lerner, G.M. and Shuster, M.D., *Magnetometer Bias Determination and Attitude Determination for Near-Earth Spacecraft*, AIAA Paper No. 79-1695, 1979.